Electronic Supplementary Material (ESI) for RSC Advances.

Electronic Supplementary Information for

Insight into Luminescent Bisazoaromatic *CNN* Pincer Palladacycle: Synthesis, Structure, Electrochemistry and Some Catalytic Applications in C–C Coupling

Sima Roy, Shuvam Pramanik, Tapas Ghorui and Kausikisankar Pramanik*

Department of Chemistry, Inorganic Chemistry Section, Jadavpur University, Kolkata – 700032, India.
E-mail: kpramanik@hotmail.com; Tel: +91 033 2457 2781

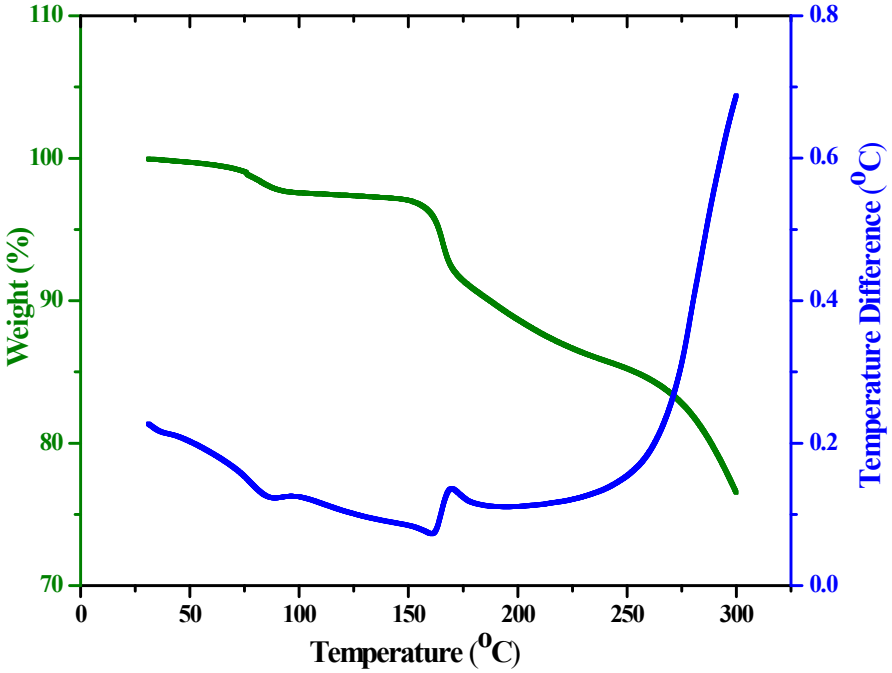

Fig. S1 TGA thermograms of complex **1**.

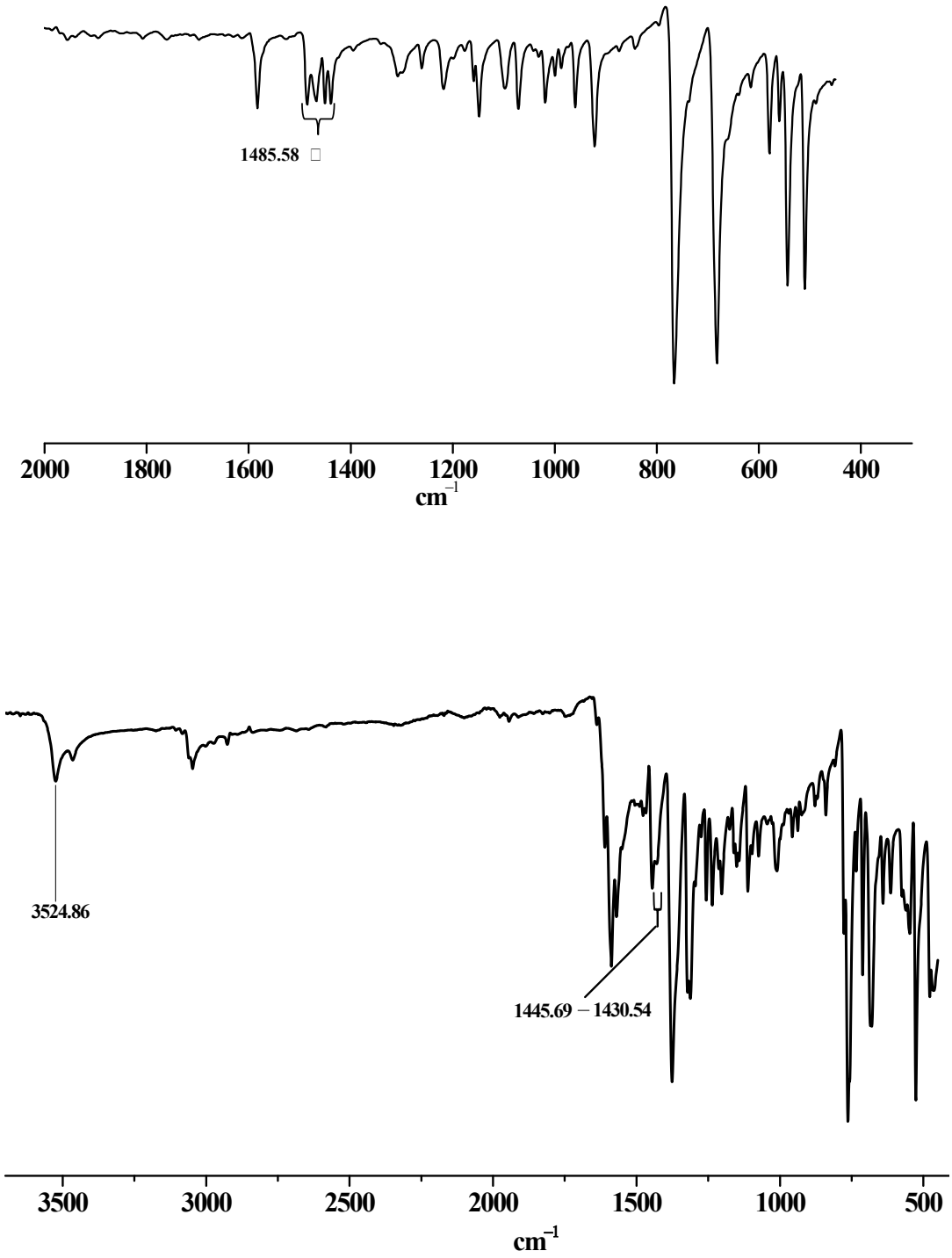

Fig. S2 FT-IR spectra of PAAB (top) and **1** (bottom)

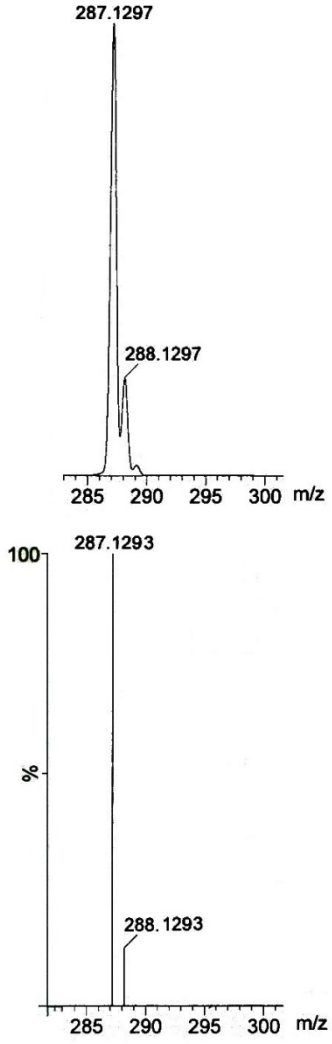

Fig. S3 ESI mass spectrum of the PAAB. Simulated isotopic pattern (top).

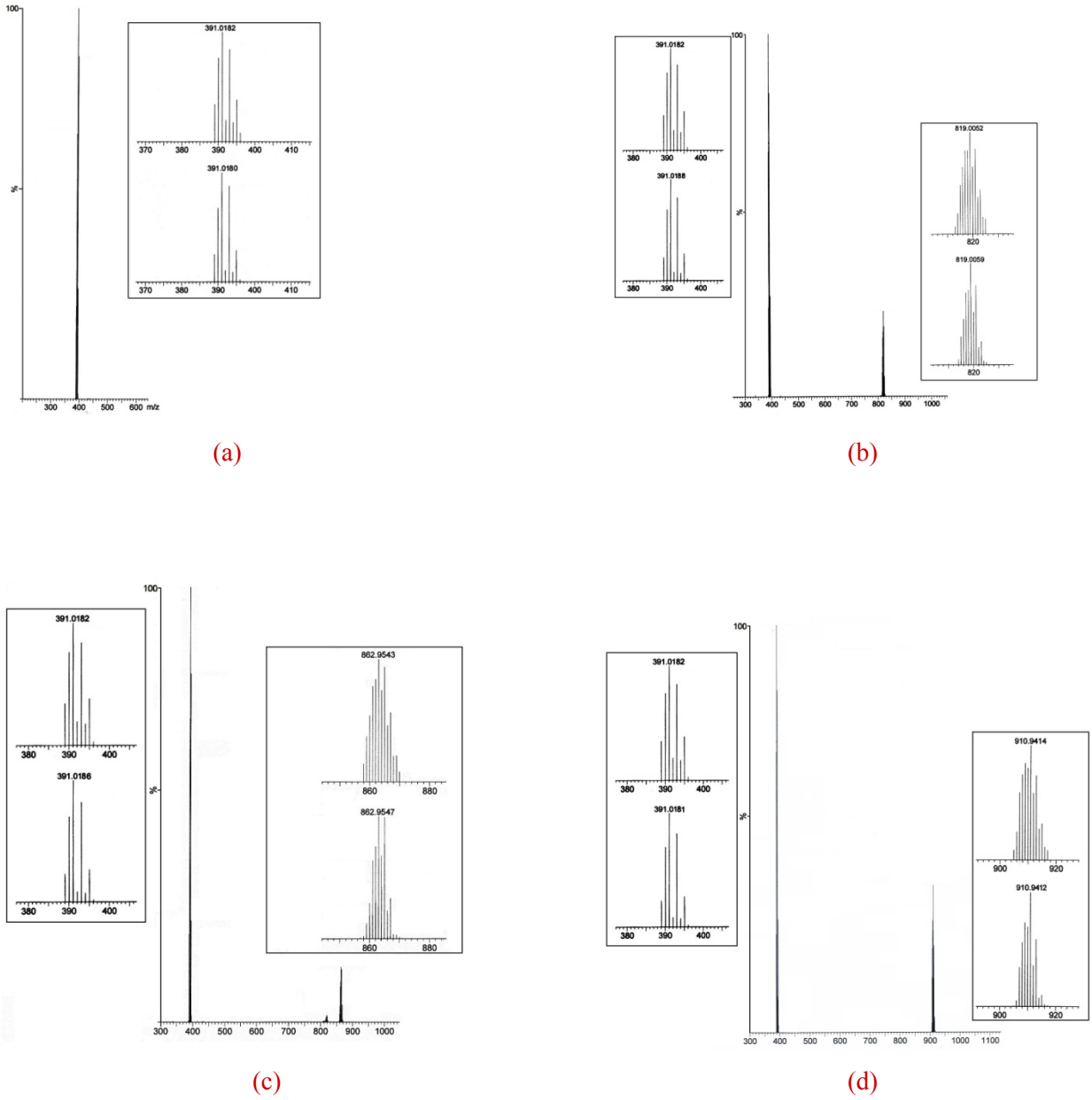

(a) (b)

(c) (d)

Fig. S4 ESI mass spectrum of the **1** (top left), **2** (top right), **3** (bottom left) and **4** (bottom right). Inset: Simulated isotopic pattern.

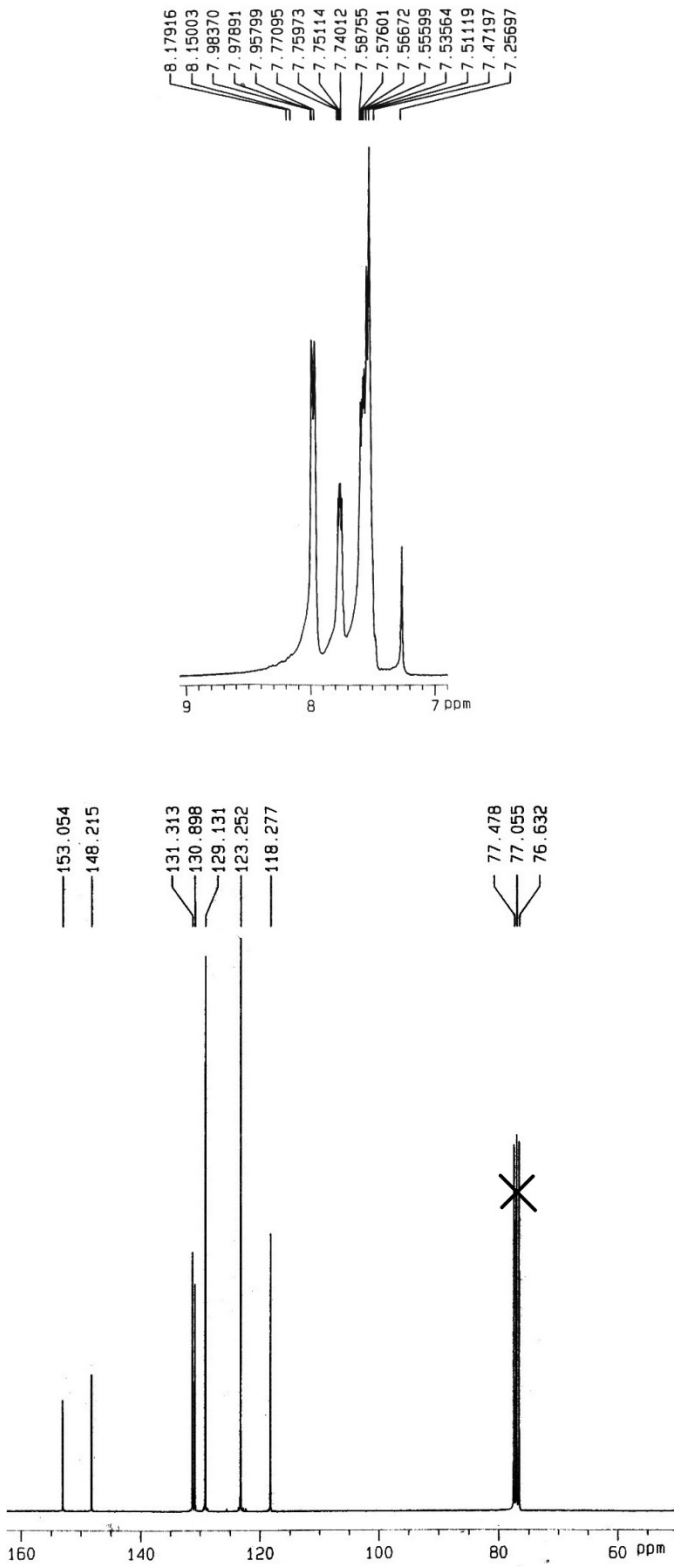

Fig. S5 Segmented ^{1}H NMR (top) and ^{13}C NMR (bottom) spectrum of PAAB.

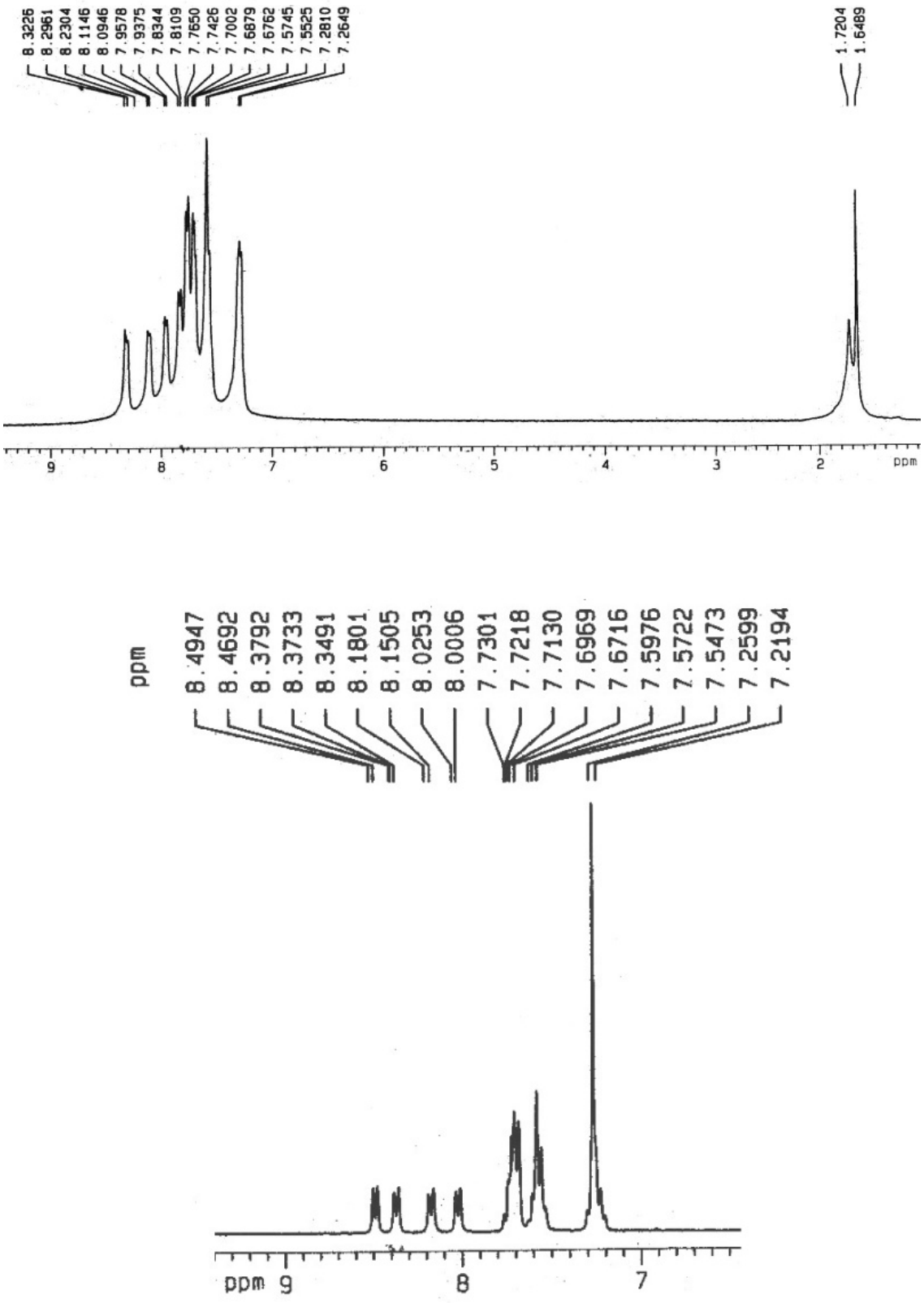

Fig. S6 ^{1}H NMR spectra of **1**(top) and **4** (bottom).

Table S1 Frontier Molecular Orbital Composition (%) in the Ground State for PAAB

Orbital	MO	Energy (EV)	Contribution (%)		Main Bond Type
			Azo	Ph (Adjacent)	
81	L + 5	−0.22	3	97	π*(Ph)
80	L + 4	−0.45	4	96	π*(Ph)
79	L + 3	−0.63	1	99	π*(Ph)
78	L + 2	−0.64	1	99	π*(Ph)
77	L + 1	−2.29	46	54	π*(Azo) + π*(Ph)
76	L	−2.85	49	51	π*(Azo) + π*(Ph)
75	H	−6.12	75	25	π(Azo) + π(Ph)
74	H – 1	−6.49	26	74	π(Azo) + π(Ph)
73	H – 2	−6.75	72	28	π(Azo) + π(Ph)
72	H – 3	−6.84	23	77	π(Azo) + π(Ph)
71	H – 4	−7.3	0	100	π(Ph)
70	H – 5	−7.31	0	100	π(Ph)
HOMO–LUMO gap = 3.27 eV					

Table S2 Frontier Molecular Orbital Composition (%) in the Ground State for **1**

Orbital	MO	Energy (EV)	Contribution (%)				Main Bond Type
			Pd	Ligand		OAc	
				Azo	Ph		
105	L + 5	–0.44	3	4	93	0	π*(Ph)
104	L + 4	–0.53	1	0	98	0	π*(Ph)
103	L + 3	–0.69	2	3	95	0	π*(Ph)
102	L + 2	–1.16	46	13	32	9	$4d_{x^2-y^2}$(Pd) + π*(Azo) + π*(Ph)
101	L + 1	–2.99	5	51	44	0	π*(Azo) + π*(Ph)
100	L	–3.42	4	50	46	0	π*(Azo) + π*(Ph)
99	H	–5.96	15	1	4	80	$4d_{z^2}$(Pd) + 2p(OAc)
98	H – 1	–6.25	24	15	31	29	$4d_{xy}$(Pd) + π(Azo)
97	H – 2	–6.54	15	5	41	38	$4d_{yz}$(Pd) + π(Ph) + 2p(OAc)
96	H – 3	–6.62	48	4	18	29	d_{z^2}(Pd) + π(Ph) + 2p(OAc)
95	H – 4	–6.88	32	24	39	4	$4d_{zx}$(Pd) + π(Azo) + π(Ph)
94	H – 5	–6.94	13	10	68	9	$4d_{zx}$(Pd) + π(Ph)
HOMO–LUMO gap = 2.54 eV							

Table S3 Frontier Molecular Orbital Composition (%) in the Ground State for **2**

Orbital	MO	Energy (EV)	Contribution (%)				Main Bond Type
			Pd	Ligand		Cl	
				Azo	Ph		
98	L+5	–0.67	4	3	93	0	π*(Ph)
97	L+4	–0.69	1	2	97	0	π*(Ph)
96	L+3	–0.9	3	7	90	0	π*(Ph)
95	L+2	–1.64	45	10	35	10	$4d_{x^2-y^2}$(Pd) + π*(Azo) + π*(Ph) + 3p(Cl)
94	L+1	–3.04	5	49	45	1	π*(Azo) + π*(Ph)
93	L	–3.46	4	47	48	1	π*(Azo) + π*(Ph)
92	H	–6.29	15	13	26	46	$4d_{xy}$(Pd) + π(Azo) + π(Ph) + 3p(Cl)
91	H–1	–6.45	26	5	12	57	$4d_{yz}$(Pd) + π(Ph) + 3p(Cl)
90	H–2	–6.59	17	7	56	20	$4d_{yz}$(Pd) + π(Ph) + 3p(Cl)
89	H–3	–6.81	82	4	2	12	$4d_{z^2}$(Pd)
88	H–4	–7	11	14	70	4	π(Azo) + π(Ph)
87	H–5	–7.16	6	12	75	7	π(Azo) + π(Ph)
HOMO–LUMO gap = 2.83 eV							

Table S4 Frontier Molecular Orbital Composition (%) in the Ground State for **3**

Orbital	MO	Energy (EV)	Contribution (%)				Main Bond Type
			Pd	Ligand		Br	
				Azo	Ph		
93	L+5	−0.67	3	2	94	0	π*(Ph)
92	L+4	−0.71	2	3	95	0	π*(Ph)
91	L+3	−0.91	2	7	90	0	π*(Ph)
90	L+2	−1.78	42	10	36	12	$4d_{x^2-y^2}$(Pd) + π*(Ph) + 4p(Br)
89	L+1	−3.07	5	48	45	1	π*(Azo) + π*(Ph)
88	L	−3.48	4	47	48	1	π*(Azo) + π*(Ph)
87	H	−6.02	10	7	14	68	π(Ph) + 4p(Br)
86	H−1	−6.18	16	2	5	77	$4d_{yz}$(Pd) + 4p(Br)
85	H−2	−6.55	15	11	68	6	$4d_{zx}$(Pd) + π(Ph)
84	H−3	−6.8	82	5	2	11	$4d_{z^2}$(Pd)
83	H−4	−6.99	14	17	68	2	$4d_{zx}$(Pd) + π(Azo) + π(Ph)
82	H−5	−7.13	8	12	76	4	π(Azo) + π(Ph)
HOMO–LUMO gap = 2.54 eV							

Table S5 Frontier Molecular Orbital Composition (%) in the Ground State for **4**

Orbital	MO	Energy (EV)	Contribution (%)				Main Bond Type
			Pd	Ligand		I	
				Azo	Ph		
93	L + 5	–0.67	4	3	93	0	π*(Ph)
92	L + 4	–0.78	3	3	94	0	π*(Ph)
91	L + 3	–0.92	2	5	93	0	π*(Ph)
90	L + 2	–1.88	39	10	36	15	$4d_{x^2-y^2}$(Pd) + π*(Ph) + 5p(I)
89	L + 1	–3.09	5	48	46	1	π*(Azo) + π*(Ph)
88	L	–3.49	3	48	48	1	π*(Azo) + π*(Ph)
87	H	–5.67	10	4	7	79	5p(I)
86	H – 1	–5.83	11	2	3	85	5p(I)
85	H – 2	–6.54	16	12	69	4	$4d_{zx}$(Pd) + π(Azo) + π(Ph)
84	H – 3	–6.74	62	6	5	28	$4d_{z^2}$(Pd) + 5p(I)
83	H – 4	–6.98	23	16	47	14	$4d_{yz}$(Pd) + π(Azo) + π(Ph) +5p(I)
82	H – 5	–7.05	22	22	53	4	$4d_{z^2}$(Pd) + π(Azo) + π(Ph)
HOMO–LUMO gap = 2.18 eV							

Table S6 Summarized Crystallographic Data for PAAB, **1**, **2**, **3** and **4**

	PAAB	**1·½H2O**	**2**	**3**	**4**
Empirical formula	$C_{18}H_{14}N_4$	$C_{40}H_{32}N_8O_4Pd_2{\cdot}H_2O$	$C_{18}H_{13}N_4ClPd$	$C_{18}H_{13}N_4BrPd$	$C_{18}H_{13}N_4IPd$
fw	286.33	919.55	427.17	471.63	518.62
T/K	296(2)	296(2)	296(2)	296(2)	296(2)
Cryst syst	Monoclinic	Monoclinic	Monoclinic	Monoclinic	Monoclinic
Space group	*P*2(1)/*c*	*P*2(1)/*n*	*C*2/*c*	*P*2(1)/*n*	*P*2(1)/*c*
a/Å	9.1369(2)	11.2390 (5)	21.9347 (6)	12.7588 (3)	9.7153(5)
b/Å	17.8053(4)	22.3058(10)	6.9520 (2)	6.8712 (2)	11.3018(5)
c/Å	9.7509(2)	15.2021 (7)	23.1894 (6)	19.0666 (5)	15.5241(7)
α /deg	90.00	90.00	90.00	90.00	90.00
β /deg	108.457(1)	104.171(2)	112.175(3)	93.257 (1)	93.107(2)
γ/deg	90.00	90.00	90.00	90.00	90.00
V/Å^3	1504.73(6)	3695.1(3)	3274.60(16)	1668.84(8)	1702.05(14)
Z	4	4	8	4	4
D_c/mgm^{-3}	1.264	1.653	1.733	1.877	2.024
μ/mm^{-1}	0.078	1.031	1.303	3.512	2.910
F(000)	600	1848	1696	920	992
cryst size/mm^3	0.58×0.45×0.22	0.44×0.35×0.21	0.38×0.32×0.16	0.52×0.43×0.23	0.36×0.24×0.14
θ/deg	2.29–27.48	1.66–27.51	2.01–27.57	1.97–28.16	2.10–29.82
measured reflns	23323	61448	26677	27890	32806
unique reflns/R_{int}	3445/ 0.0285	8482/0.0351	3758 /0.0386	4072 / 0.0325	4791 / 0.0506
GOF on F^2	1.041	1.015	1.025	1.028	1.047
R1,[a] wR2[b] [$I > 2\sigma(I)$]	0.0407, 0.1059	0.0278, 0.0666	0.0270, 0.0626	0.0273, 0.0655	0.0413, 0.0964
R1, wR2 (all data)	0.0536, 0.1159	0.0428, 0.0745	0.0353,0.0675	0.0410, 0.0719	0.0564, 0.1101

[a]$R1 = \Sigma||F_o| - |F_c||/\Sigma|F_o|$. [b]$wR2 = [\Sigma w(F_o^2 - F_c^2)^2/\Sigma w(F_o^2)^2]^{1/2}$.

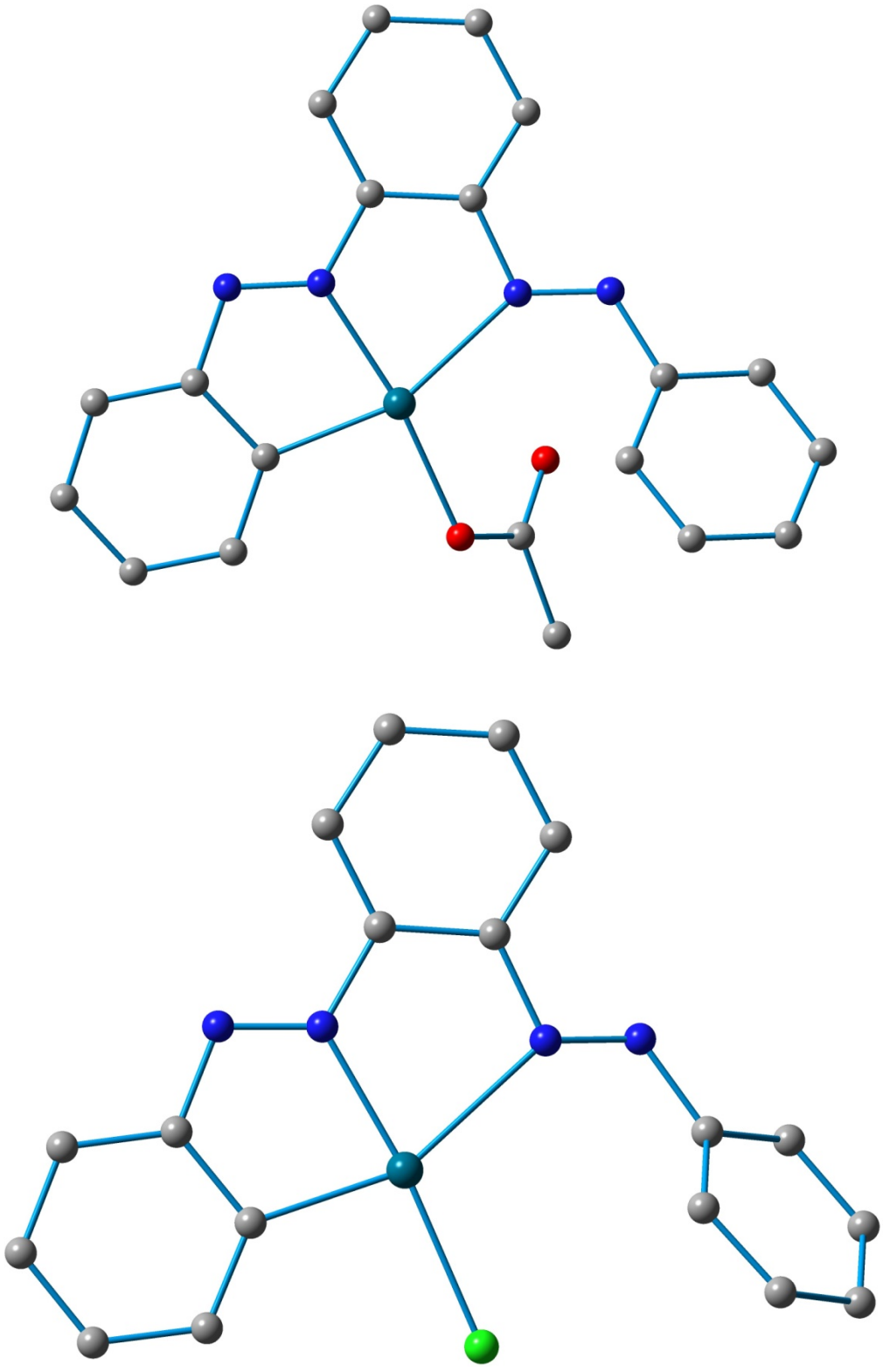

Fig. S7 Optimized molecular structures of **1** and **2** (Pd: cyan, N: blue, O: red, C: grey. Hydrogen atoms are omitted for clarity).

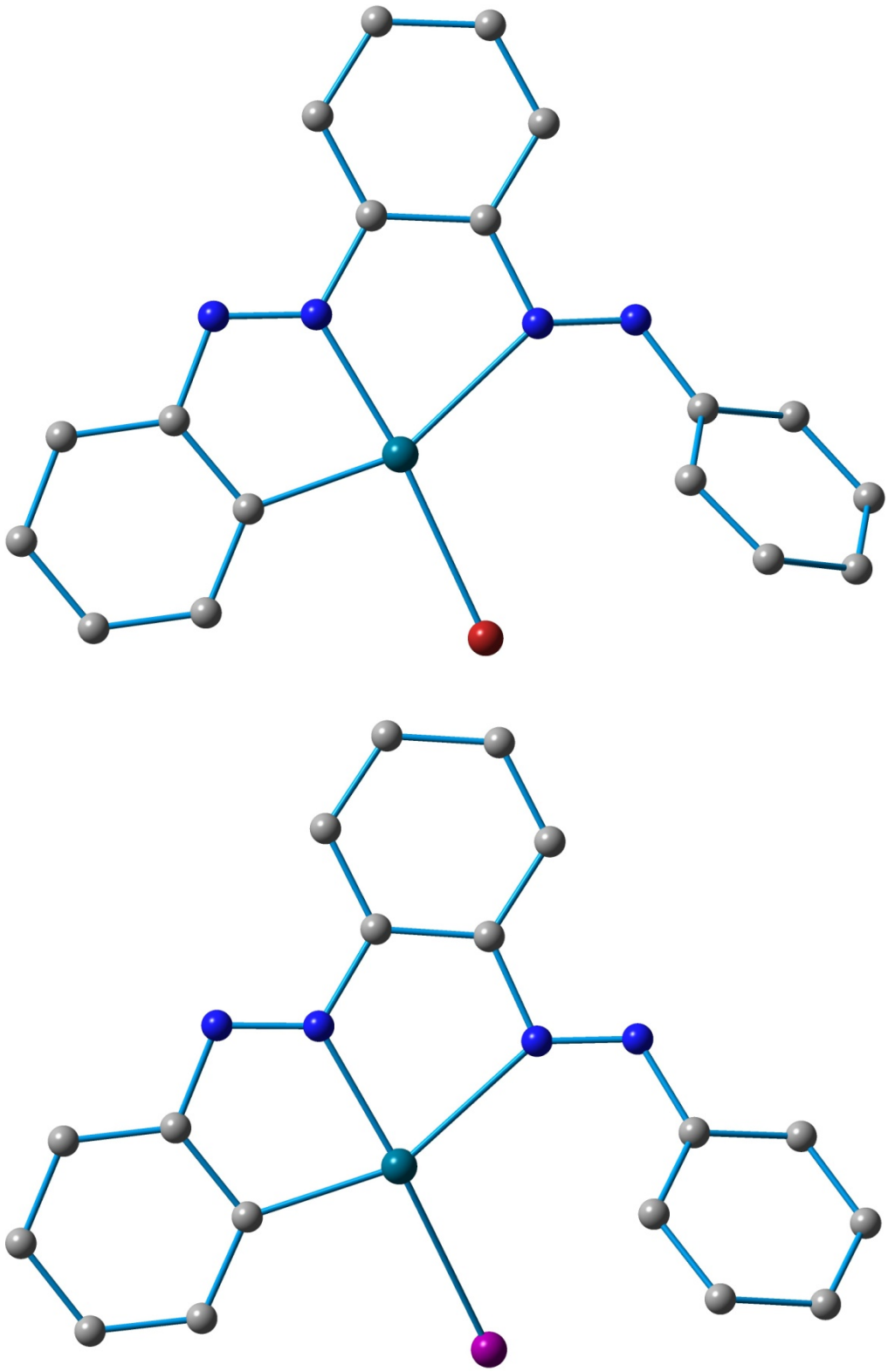

Fig. S8 Optimized molecular structures of **3** and **4** (Pd: cyan, N: blue, O: red, C: grey. Hydrogen atoms are omitted for clarity).

Table S7 Selected optimized geometrical parameters of **1**, **2**, **3** and **4** in the ground and lower lying triplet excited states at B3LYP level

Bond Lengths (Å)							
1		**2**		**3**		**4**	
	S_0		S_0		S_0		S_0
Pd1–C38	1.99128	Pd1–C6	1.98633	Pd1–C6	1.99299	Pd1–C7	1.99727
Pd1–N4	2.00045	Pd1–N2	2.01489	Pd1–N2	2.01993	Pd1–N3	2.02657
Pd1–N5	2.26044	Pd1–N4	2.34821	Pd1–N4	2.35192	Pd1–N5	2.34329
Pd1–O2	2.06773	Pd1–Cl37	2.34217	Pd1–Br37	2.50980	Pd1–I2	2.66900
N4–N7	1.29511	N2–N3	1.26999	N2–N3	1.26920	N3–N4	1.26924
N5–N6	1.27759	N4–N5	1.25902	N4–N5	1.25909	N5–N6	1.25658
Bond Angles (°)							
C38–Pd1–N4	79.477	C6–Pd1–N2	79.003	C6–Pd1–N2	78.953	C7–Pd1–N3	78.960
C38–Pd1–N5	158.213	C6–Pd1–N4	155.974	C6–Pd1–N4	155.940	C7–Pd1–N5	155.551
C38–Pd1–O2	91.882	C6–Pd1–Cl37	94.607	C6–Pd1–Br37	94.992	C7–Pd1–I2	96.443
N4–Pd1–N5	78.872	N2–Pd1–N4	77.285	N2–Pd1–N4	77.120	N3–Pd1–N5	76.782
N4–Pd1–O2	170.638	N2–Pd1–Cl37	173.602	N2–Pd1–Br37	173.463	N3–Pd1–I2	168.229
N5–Pd1–O2	109.877	N4–Pd1–Cl37	109.066	N4–Pd1–Br37	108.793	N5–Pd1–I2	107.954

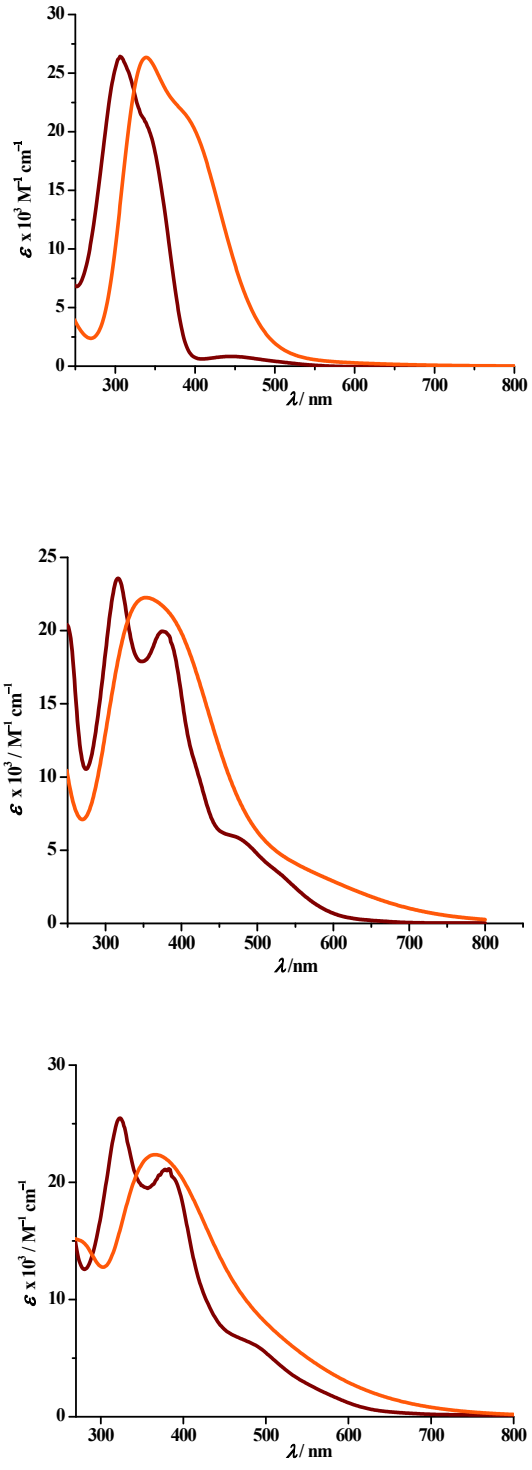

Fig. S9 Experimental (wine red) and theoretical (orange) absorption spectra of PAAB (top), **1** (middle) and **3** (bottom).

Table S8 Main optical transition at the TD-DFT/B3LYP/6-311+G(d,p) + LANL2DZ Level for the complex **1** with composition in terms of molecular orbital contribution of the transition, Computed Vertical excitation energies, and oscillator strength in dichloromethane

Transition	CI	Composition	E (eV)	Oscillator strength (*f*)	λ_{theo} (nm)
$S_0 \rightarrow S_2$	0.64389	H → L	2.1354	0.0730	580.62
$S_0 \rightarrow S_3$	0.50564 0.33856	H → L + 1 H − 2 → L	2.4585	0.0459	504.31
$S_0 \rightarrow S_5$	0.53378 -0.33752	H − 2 → L H → L + 1	2.6842	0.0673	461.90
$S_0 \rightarrow S_7$	0.39797 0.37913 0.29778	H − 4 → L H − 3 → L H − 5 → L	2.8188	0.0337	439.85
$S_0 \rightarrow S_8$	0.57535 -0.25813	H − 5 → L H − 3 → L	3.0083	0.1340	412.15
$S_0 \rightarrow S_9$	0.52991	H − 2 → L + 1	3.0495	0.2422	406.58
$S_0 \rightarrow S_{11}$	0.56424 0.25095	H − 3 → L + 1 H − 4 → L + 1	3.1801	0.0233	389.88
$S_0 \rightarrow S_{12}$	0.49480 -0.35480	H − 7 → L H − 4 → L + 1	3.2541	0.0273	381.01
$S_0 \rightarrow S_{13}$	0.40942 -0.36600 -0.27554	H − 6 → L H − 5 → L + 1 H − 4 → L + 1	3.2966	0.1139	376.10
$S_0 \rightarrow S_{15}$	0.46450 -0.32367 0.24513	H − 5 → L + 1 H − 8 → L H − 6 → L	3.4853	0.1492	355.73
$S_0 \rightarrow S_{17}$	0.42639 -0.29320 0.27910	H → L + 2 H − 6 → L + 1 H − 1 → L + 2	3.6621	0.0629	338.56
$S_0 \rightarrow S_{20}$	0.53680 0.26820	H − 7 → L + 1 H → L + 2	3.8130	0.1829	325.16
$S_0 \rightarrow S_{23}$	0.52098 0.29931	H − 9 → L + 1 H − 2 → L + 2	4.0476	0.1464	306.32

Table S9 Main optical transition at the TD-DFT/B3LYP/6-311+G(d,p) + LANL2DZ Level for the complex **2** with composition in terms of molecular orbital contribution of the transition, Computed Vertical excitation energies, and oscillator strength in dichloromethane

Transition	CI	Composition	E (ev)	Oscillator strength (*f*)	λ_{theo} (nm)
$S_0 \rightarrow S_1$	0.58265 0.32421	H → L H – 1 → L	2.2055	0.0420	562.17
$S_0 \rightarrow S_2$	0.42144 0.31999 –0.30584 0.23013	H – 1 → L H – 3 → L H → L H – 2 → L	2.3803	0.0700	520.88
$S_0 \rightarrow S_3$	0.37165 –0.33790 –0.30434 0.25011	H – 1 → L H – 3 → L H – 2 → L H → L+1	2.5421	0.0669	487.72
$S_0 \rightarrow S_4$	0.23310 0.54832	H – 2 → L H → L+1	2.7030	0.0374	458.69
$S_0 \rightarrow S_6$	0.49021 0.35571	H – 1 → L+1 H – 3 → L+1	2.9146	0.0743	425.38
$S_0 \rightarrow S_7$	0.58353 –0.23628	H – 4 → L H → L+1	2.9382	0.0454	421.97
$S_0 \rightarrow S_8$	0.36634 0.31859 –0.28319 0.27378	H – 3 → L+1 H – 2 → L+1 H – 1 → L+1 H – 4 → L	3.0771	0.1594	402.93
$S_0 \rightarrow S_9$	0.44979 –0.37349 0.26382	H – 5 → L H – 6 → L H – 3 → L+1	3.1546	0.0851	393.02
$S_0 \rightarrow S_{10}$	0.43479 0.36515 –0.28927	H – 2 → L+1 H – 5 → L H – 3 → L+1	3.1728	0.0896	390.77
$S_0 \rightarrow S_{11}$	0.41964 –0.33515 0.27115 –0.22019	H – 6 → L H – 2 → L+1 H – 5 → L H – 4 → L+1	3.2358	0.1378	383.16
$S_0 \rightarrow S_{12}$	0.48613 0.29071	H – 4 → L+1 H → L+2	3.3843	0.0381	366.35
$S_0 \rightarrow S_{13}$	0.35228 –0.25906 –0.22170	H → L+2 H – 4 → L+1 H – 5 → L+1	3.4862	0.0208	355.64
$S_0 \rightarrow S_{20}$	0.45436 –0.43054	H – 2 → L+2 H – 3 → L+2	3.7788	0.0296	328.11

Table S10 Main optical transition at the TD-DFT/B3LYP/6-311+G(d,p) + LANL2DZ Level for the complex **3** with composition in terms of molecular orbital contribution of the transition, Computed Vertical excitation energies, and oscillator strength in dichloromethane

Transition	**CI**	**Composition**	**E (ev)**	**Oscillator strength (*f*)**	λ_{theo} **(nm)**
$S_0 \rightarrow S_1$	0.66332	H → L	2.1002	0.0380	590.35
$S_0 \rightarrow S_2$	0.53292 –0.24871 0.22793	H – 3 → L H – 2 → L H – 1 → L	2.3660	0.0353	524.02
$S_0 \rightarrow S_3$	0.58824 0.22812	H – 1 → L H – 2 → L	2.4642	0.0685	503.15
$S_0 \rightarrow S_5$	0.58883 0.22220	H – 2 → L H – 3 → L	2.5889	0.0498	478.91
$S_0 \rightarrow S_6$	0.52804	H – 4 → L	2.8228	0.0943	439.22
$S_0 \rightarrow S_9$	0.48028 0.36967 –0.25643	H – 3 → L + 1 H – 2 → L + 1 H – 1 → L + 1	3.0119	0.0342	411.65
$S_0 \rightarrow S_{10}$	0.55043 0.28621	H – 5 → L H – 6 → L	3.1056	0.2751	399.23
$S_0 \rightarrow S_{11}$	0.43840 –0.33515	H – 6 → L H – 5 → L	3.1464	0.1047	394.05
$S_0 \rightarrow S_{13}$	0.41413 –0.28247 –0.28551	H → L + 2 H – 8 → L H – 4 → L + 1	3.3197	0.0404	373.48
$S_0 \rightarrow S_{14}$	0.42349 0.33132 0.26713	H – 3 → L + 2 H – 8 → L H – 5 → L + 1	3.4172	0.0390	362.83
$S_0 \rightarrow S_{17}$	0.54526 0.28212	H – 7 → L H – 5 → L + 1	3.5598	0.0553	348.29
$S_0 \rightarrow S_{18}$	0.37667 0.35524 –0.27182	H – 5 → L + 1 H – 2 → L + 2 H – 7 → L	3.5638	0.1200	347.89
$S_0 \rightarrow S_{19}$	0.35655 –0.34973 0.25212	H – 5 → L + 1 H – 2 → L + 2 H – 6 → L + 1	3.6277	0.1789	341.77
$S_0 \rightarrow S_{20}$	0.49643 0.22922	H – 6 → L + 1 H – 2 → L + 2	3.6565	0.1182	339.08
$S_0 \rightarrow S_{23}$	0.43538 0.40861 –0.22664	H – 8 → L + 1 H – 7 → L + 1 H – 10 → L	3.9762	0.0714	311.82

Table S11 Main optical transition at the TD-DFT/B3LYP/6-311+G(d,p) + LANL2DZ Level for the complex **4** with composition in terms of molecular orbital contribution of the transition, Computed Vertical excitation energies, and oscillator strength in dichloromethane

Transition	CI	Composition	E (ev)	Oscillator strength (*f*)	λ_{theo} (nm)
$S_0 \rightarrow S_1$	0.68277	H → L	1.8970	0.0257	653.59
$S_0 \rightarrow S_4$	0.55718 –0.25694	H – 3 → L H – 2 → L	2.4414	0.0347	507.84
$S_0 \rightarrow S_5$	0.58351 0.25534	H – 2 → L H – 3 → L	2.4631	0.0921	503.36
$S_0 \rightarrow S_6$	0.65540	H – 1 → L+1	2.6448	0.0340	468.79
$S_0 \rightarrow S_7$	0.49816 –0.21876	H – 4 → L H – 2 → L+1	2.7640	0.0631	448.58
$S_0 \rightarrow S_{10}$	0.51434 0.38058	H – 3 → L+1 H – 2 → L+1	2.9500	0.0285	420.29
$S_0 \rightarrow S_{12}$	0.50322 0.36638	H – 5 → L H – 6 → L	3.0617	0.3490	404.95
$S_0 \rightarrow S_{14}$	0.40278 –0.31232	H – 4 → L+1 H – 1 → L+2	3.2074	0.0377	386.55
$S_0 \rightarrow S_{15}$	0.39231 –0.36445 –0.31185	H – 7 → L H – 5 → L+1 H – 4 → L+1	3.3218	0.0463	373.24
$S_0 \rightarrow S_{17}$	0.32311 –0.30191 –0.30110 –0.29412	H – 6 → L+1 H – 8 → L H – 7 → L H – 5 → L+1	3.4252	0.0496	361.98
$S_0 \rightarrow S_{18}$	0.42580 –0.25519 0.32929	H – 2 → L+2 H – 8 → L H – 6 → L+1	3.4725	0.0368	357.05
$S_0 \rightarrow S_{19}$	0.42694 –0.32566 –0.26389	H – 8 → L H – 5 → L+1 H – 7 → L	3.5345	0.0555	350.79
$S_0 \rightarrow S_{20}$	0.39681 0.31536 –0.02799 –0.23494	H – 6 → L+1 H – 5 → L+1 H – 8 → L H – 4 → L+1	3.5619	0.2726	348.08
$S_0 \rightarrow S_{22}$	0.39166 0.36962 –0.35894	H – 10 → L H – 9 → L H – 7 → L+1	3.7728	0.1017	328.63

		Hole	Electron
530 nm	S_2 w = 0.36 2.3803 (0.0700) 523.88 MLCT/LLCT $4d_{zx}$(Pd) + 3p(Cl) → π*(azo + Ph)		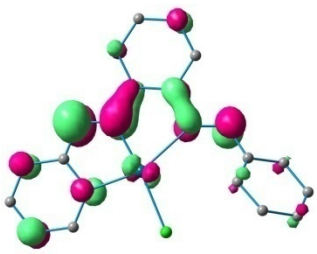
480 nm	S_3 w = 0.28 2.5421 (0.0669) 487.72 MLCT/LLCT $4d_{zx}$(Pd) + 3p(Cl) → π*(azo + Ph)	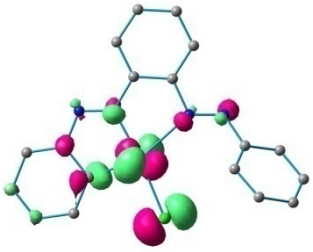	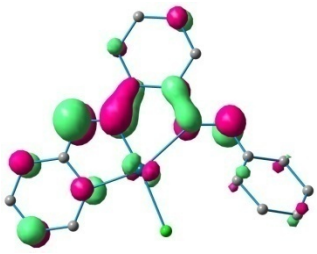
381 nm	S_{11} w = 0.35 3.2358 (0.1378) 383.16 ILCT/MLCT π(Ph) + $4d_z^2$(Pd) → π*(azo + Ph)	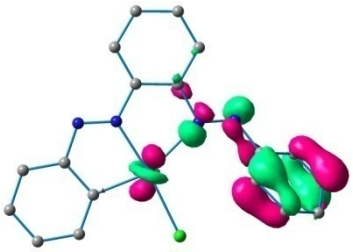	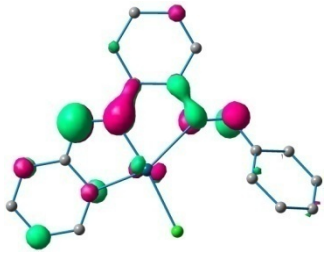
323 nm	S_{19} w = 0.55 3.7132 (0.2195) 333.90 ILCT/MLCT π(Ph + azo) + $4d_z^2$(Pd) → π*(azo + Ph)	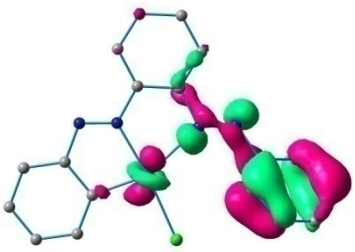	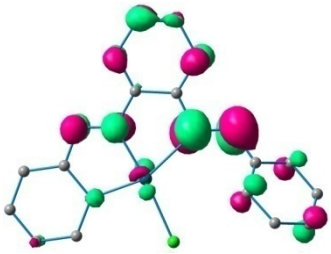

Fig. S10 Natural transition orbitals (NTOs) for complex **2** illustrating the nature of singlet excited states in the absorption bands in the range 250–700 nm. For each state, the respective number of the state, transition energy (eV), and the oscillator strength (in parentheses) are listed. Shown are only occupied (holes) and unoccupied (electrons) NTO pairs that contribute more than 25% to each excited state.

		Hole	Electron
560 nm	S_1 w = 0.88 2.1002 (0.0380) 590.35 LLCT/ MLCT/ILCT 4p(Br) + $4d_{xy}$(Pd) + π(azo) → π*(azo + Ph)	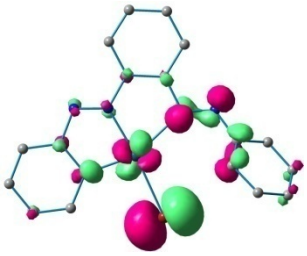	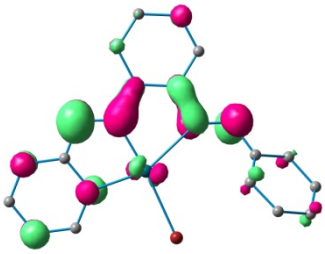
	S_2 w = 0.57 2.3660 (0.0353) 524.02 MLCT $4d_z^2$(Pd) → π*(azo + Ph)	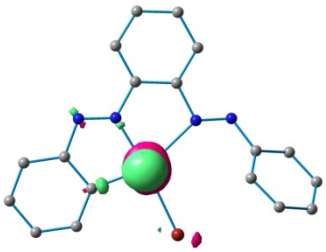	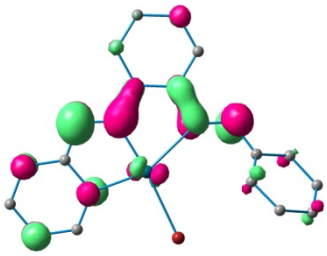
490 nm	S_3 w = 0.69 2.4642 (0.0685) 503.15 LLCT/MLCT/ILCT 4p(Br) + $4d_z^2$(Pd) + π(Ph) → π*(azo + Ph)	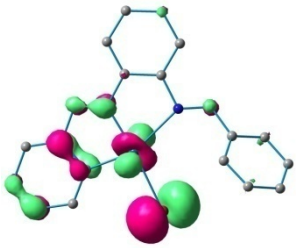	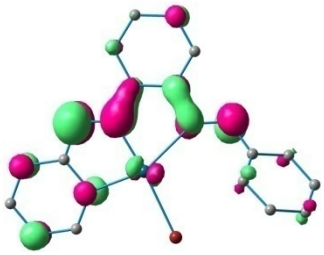
377 nm	S_{11} w = 0.35 3.2358 (0.1378) 383.16 ILCT/MLCT π(Ph) + $4d_z^2$(Pd) → π*(azo)	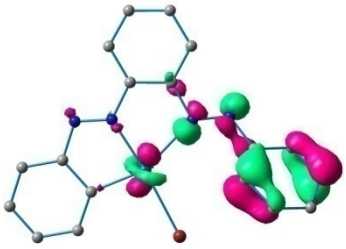	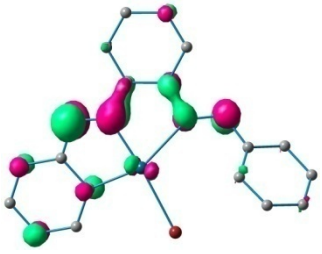
318 nm	S_{23} w = 0.34 3.9762(0.0714) 311.82 ILCT/LLCT π(Ph + azo) + 4p(Br) → π*(azo + Ph)	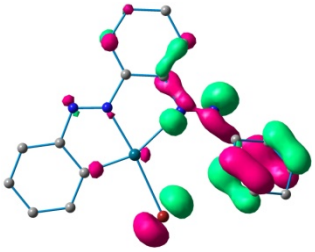	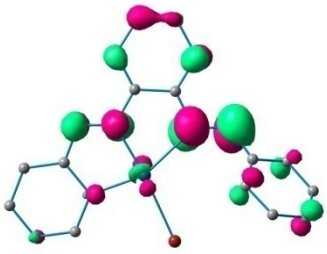

Fig. S11 Natural transition orbitals (NTOs) for complex **3** illustrating the nature of singlet excited states in the absorption bands in the range 250–700 nm. For each state, the respective number of the state, transition energy (eV), and the oscillator strength (in parentheses) are listed. Shown are only occupied (holes) and unoccupied (electrons) NTO pairs that contribute more than 25% to each excited state.

		Hole	Electron
600 nm	S_1 w = 0.93 1.8970 (0.0257) 653.59 LLCT 5p(I) → π*(azo + Ph)	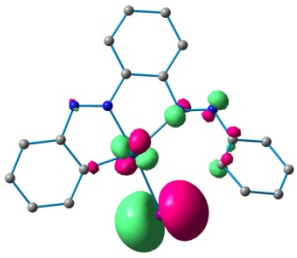	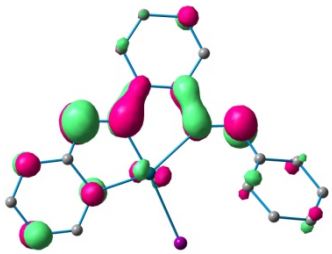
500 nm	S_4 w = 0.62 2.4414 (0.0347) 507.84 MLCT $4d_{Z^2}$(Pd) → π*(azo + Ph)	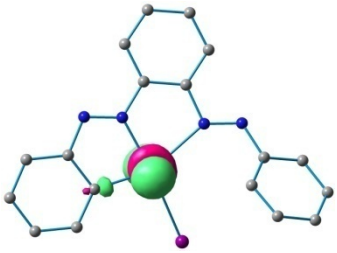	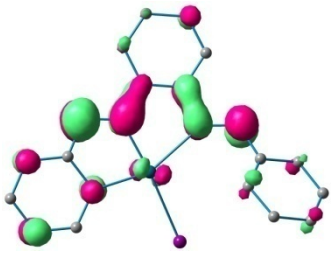
	S_5 w = 0.68 2.4631 (0.0921) 503.36 ILCT/MLCT π(Ph) + $4d_{zx}$(Pd) → π*(azo + Ph)	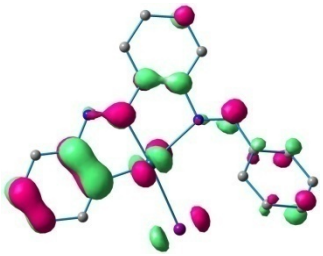	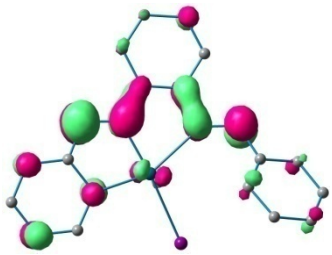
382 nm	S_{14} w = 0.35 3.2074 (0.0377) 386.55 ILCT/MLCT π(Ph) + $4d_{z^2}$(Pd) → π*(azo + Ph)	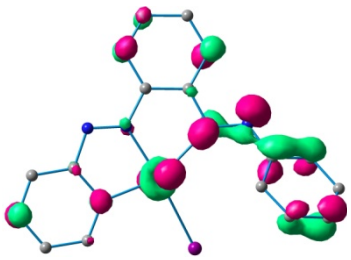	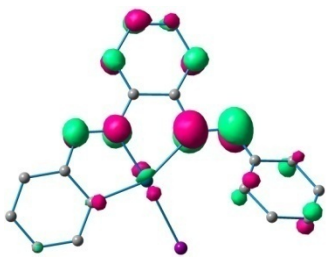
334 nm	S_{20} w = 0.32 3.5619 (0.2726) 348.08 LLCT/ILCT π(Ph) + 5p(I) → π*(azo + Ph)	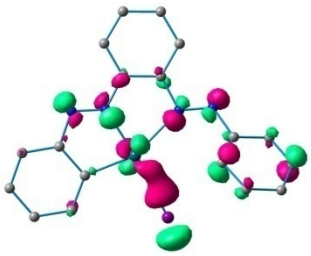	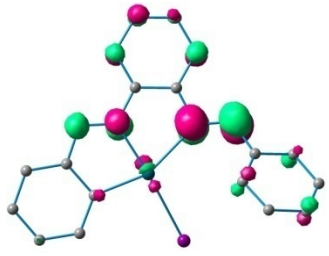

Fig. S12 Natural transition orbitals (NTOs) for complex **4** illustrating the nature of singlet excited states in the absorption bands in the range 250–700 nm. For each state, the respective number of the state, transition energy (eV), and the oscillator strength (in parentheses) are listed. Shown are only occupied (holes) and unoccupied (electrons) NTO pairs that contribute more than 25% to each excited state.

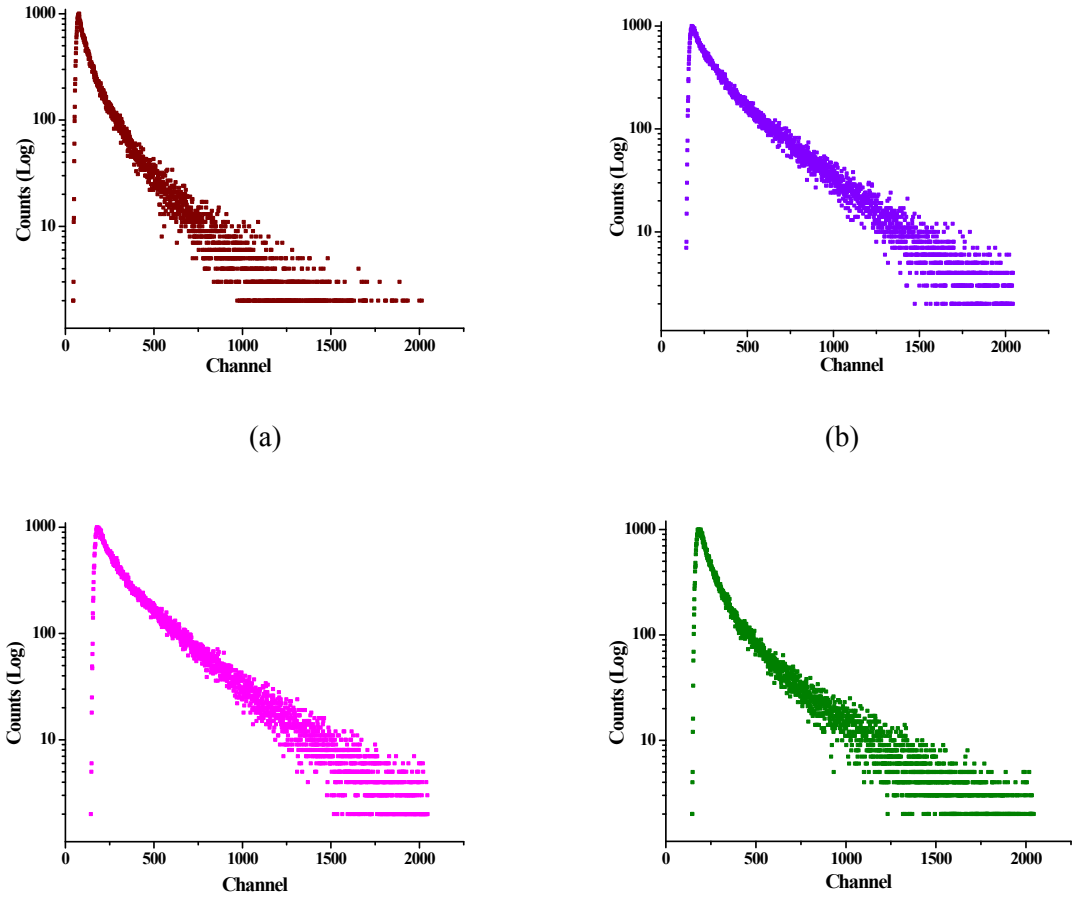

Fig. S13 Changes in the time-resolved photoluminescence decay of complexes **1** (a), **2** (b), **3** (c) and **4** (d) obtained with excitation at 300 nm. The emission at 352 nm was monitored.

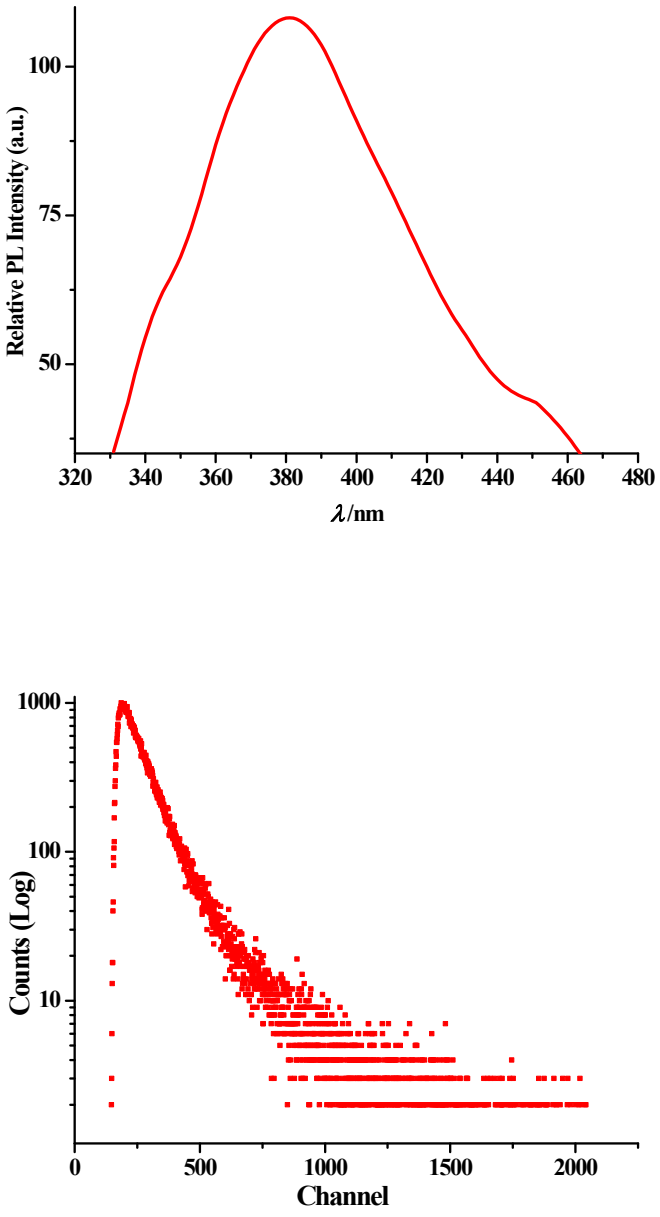

Fig. S14 Luminescence spectrum and changes in the time-resolved photoluminescence decay of ligand PAAB obtained with excitation at 300 nm. The emission at 384 nm was monitored.

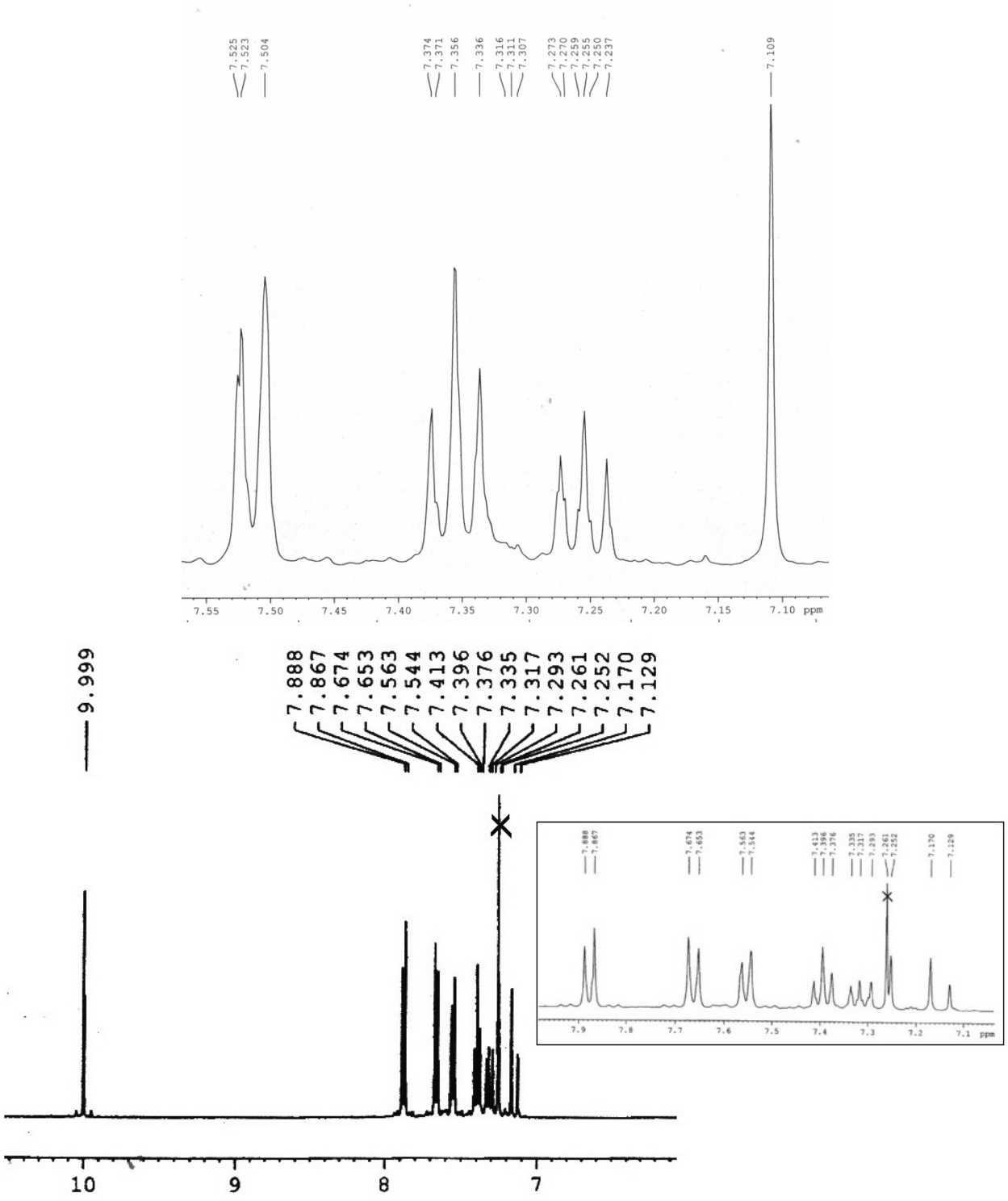

Fig. S15 ^{1}H NMR spectra of **8** (top) and **9** (bottom)

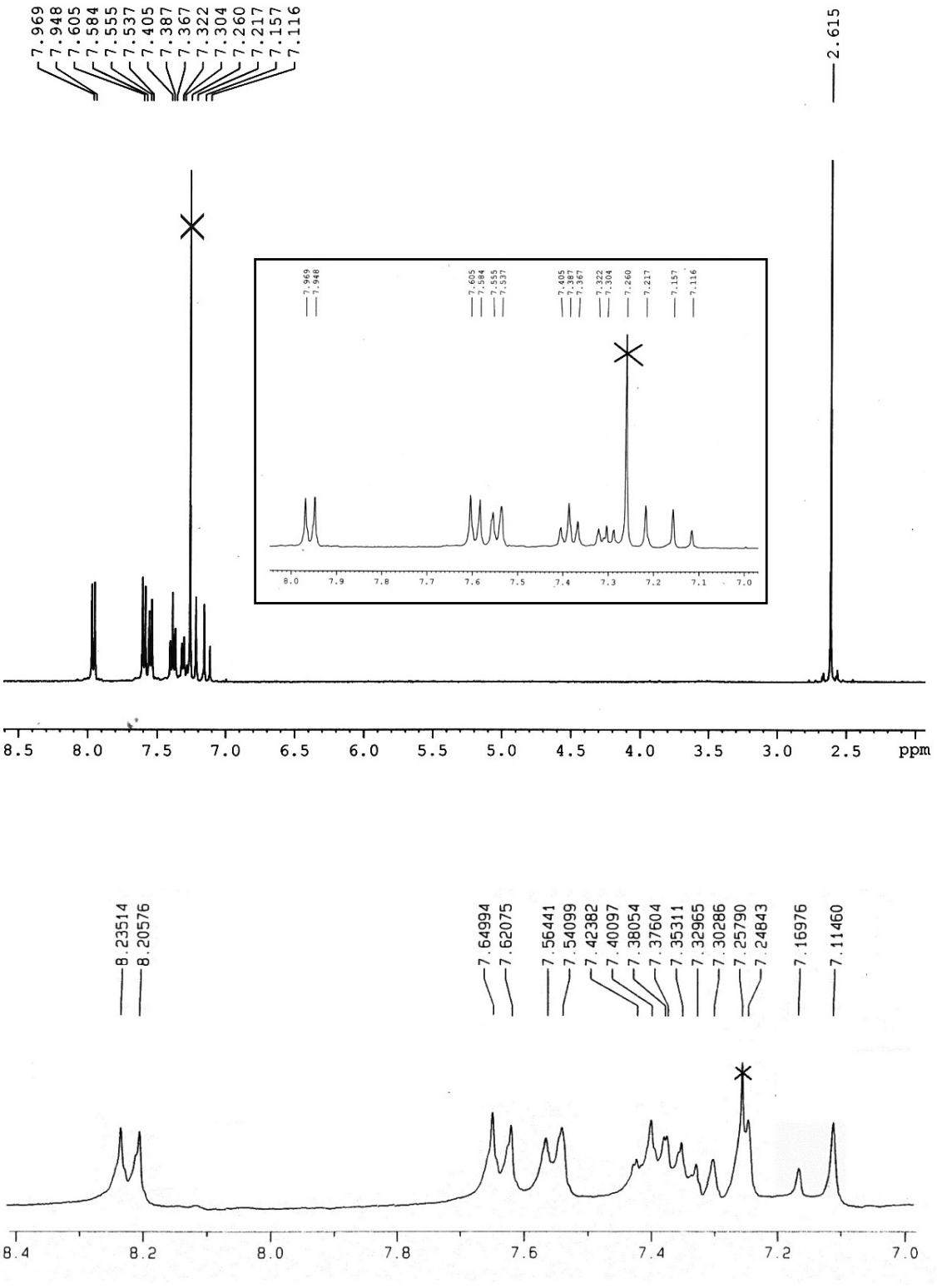

Fig. S16 ^{1}H NMR spectra of **10** (top) and **11** (bottom)

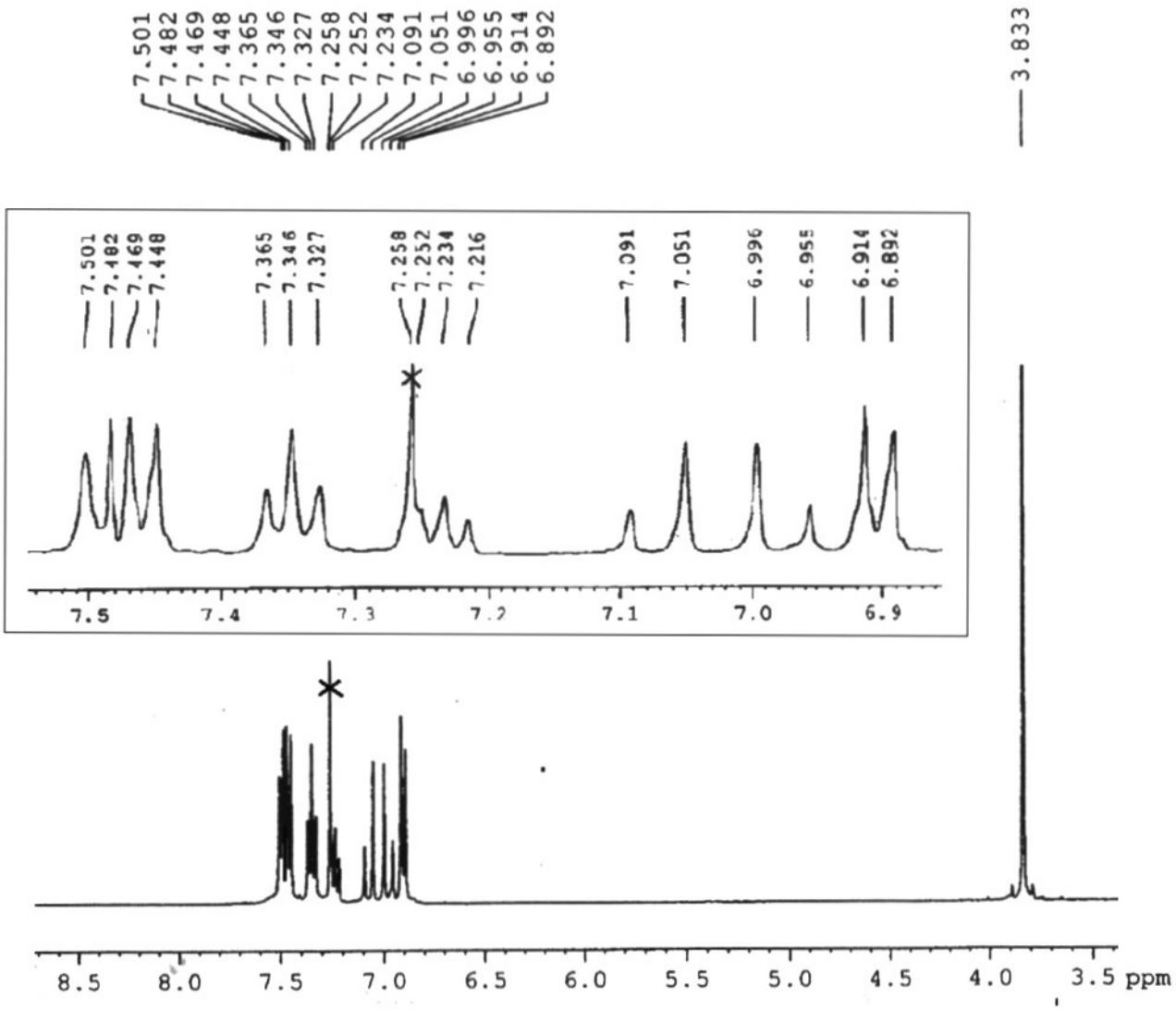

Fig. S17 ^{1}H NMR spectra of **12**

Table S12 Coordinates of optimized geometry **[1]1**

Tag	Symbol	X	Y	Z
1	Pd	8.269446	18.56174	9.407978
2	O	8.102663	20.59595	9.076791
3	O	5.859774	20.35533	9.412311
4	N	8.469592	16.57133	9.404958
5	N	7.31643	18.02443	11.38602
6	N	6.749863	18.62936	12.35828
7	N	9.06783	15.98577	8.416766
8	C	7.824714	15.83519	10.41476
9	C	7.189296	16.58581	11.42984
10	C	6.935034	20.01218	12.55353
11	C	8.06955	20.73038	12.13866
12	H	8.847923	20.24124	11.576
13	C	8.185008	22.07684	12.47331
14	H	9.060329	22.62887	12.16071
15	C	7.17622	22.71456	13.2053
16	H	7.272289	23.76238	13.45598
17	C	6.05076	21.99575	13.62618
18	H	5.274504	22.48634	14.19665
19	C	5.939232	20.64379	13.32013
20	H	5.092105	20.05817	13.64596
21	C	6.499959	15.91262	12.44806
22	H	6.023171	16.49796	13.21745
23	C	6.446281	14.523	12.45167
24	H	5.909429	14.01127	13.23824
25	C	7.08607	13.78227	11.44375
26	H	7.042682	12.70218	11.45578
27	C	7.772867	14.43378	10.42711
28	H	8.266136	13.89293	9.634591
29	C	9.539059	16.91163	7.48499
30	C	10.25322	16.47059	6.356996
31	H	10.43938	15.41368	6.227392
32	C	10.69881	17.41229	5.4362
33	H	11.25127	17.09591	4.56246
34	C	10.42969	18.77705	5.639562
35	H	10.78246	19.5005	4.915519
36	C	9.711579	19.21934	6.760858
37	H	9.503974	20.26872	6.913162
38	C	9.25904	18.29835	7.700192
39	C	6.85069	21.05834	9.10468
40	C	6.719577	22.51432	8.717695
41	H	5.703561	22.85413	8.899697
42	H	6.955698	22.63785	7.658747
43	H	7.424951	23.12384	9.282425

Table S13 Coordinates of optimized geometry **^{1}2**

Tag	Symbol	X	Y	Z
1	Pd	5.981088	9.798353	1.003808
2	N	6.343946	10.67829	-0.77209
3	N	5.783056	10.2376	-1.82284
4	N	7.570054	11.43737	1.554172
5	N	8.44014	11.6064	2.448327
6	C	4.876468	8.676752	-0.20754
7	C	4.076231	7.570011	0.040752
8	H	3.986981	7.188683	1.049413
9	C	3.384085	6.960261	-1.01235
10	H	2.756021	6.100979	-0.80134
11	C	3.480486	7.434061	-2.32605
12	H	2.934854	6.942276	-3.1225
13	C	4.278235	8.533143	-2.60267
14	H	4.382369	8.924084	-3.60789
15	C	4.97406	9.152273	-1.5506
16	C	7.220445	11.77088	-0.84845
17	C	7.470499	12.46095	-2.04158
18	H	6.96254	12.14102	-2.94117
19	C	8.352863	13.52829	-2.04603
20	H	8.540955	14.06688	-2.96736
21	C	8.992965	13.91645	-0.86228
22	H	9.673483	14.75987	-0.86616
23	C	8.752673	13.23598	0.32164
24	H	9.232453	13.53302	1.24376
25	C	7.869691	12.14826	0.34514
26	C	8.196059	11.15341	3.748999
27	C	6.920566	11.05913	4.324057
28	H	6.043665	11.28877	3.736714
29	C	6.802549	10.7029	5.661597
30	H	5.81834	10.63191	6.108307
31	C	7.938034	10.42081	6.419942
32	H	7.833936	10.13456	7.460417
33	C	9.21029	10.51768	5.848859
34	H	10.0917	10.30451	6.442121
35	C	9.34253	10.90733	4.525107
36	H	10.31626	11.01723	4.062914
37	Cl	5.415651	8.601533	2.936081

Table S14 Coordinates of optimized geometry **[1]3**

Tag	Symbol	X	Y	Z
1	Pd	6.05001	9.718522	0.990721
2	N	6.325519	10.68042	-0.76398
3	N	5.729561	10.27286	-1.80782
4	N	7.603314	11.39382	1.549441
5	N	8.457772	11.58813	2.45357
6	C	4.904234	8.631384	-0.22473
7	C	4.119543	7.506255	-0.00429
8	H	4.071986	7.067843	0.983189
9	C	3.38657	6.944717	-1.05671
10	H	2.773501	6.07106	-0.86125
11	C	3.424101	7.482878	-2.34774
12	H	2.848549	7.027412	-3.14468
13	C	4.203874	8.600049	-2.59984
14	H	4.265539	9.042137	-3.58718
15	C	4.938937	9.172233	-1.54767
16	C	7.212225	11.76436	-0.84041
17	C	7.444056	12.47016	-2.02844
18	H	6.910152	12.17202	-2.9204
19	C	8.343104	13.52303	-2.03804
20	H	8.518049	14.07288	-2.95531
21	C	9.018742	13.88111	-0.86433
22	H	9.714146	14.71227	-0.87202
23	C	8.794563	13.18728	0.314531
24	H	9.300004	13.46311	1.229353
25	C	7.894425	12.11305	0.343417
26	C	8.201476	11.15414	3.757288
27	C	6.918385	11.07574	4.31787
28	H	6.050755	11.29165	3.710977
29	C	6.78231	10.76352	5.664747
30	H	5.792662	10.709	6.101625
31	C	7.907006	10.5013	6.445241
32	H	7.789045	10.24777	7.49265
33	C	9.186647	10.5759	5.887001
34	H	10.05973	10.3769	6.497212
35	C	9.337119	10.92789	4.554904
36	H	10.31718	11.02417	4.103197
37	Br	5.632661	8.29519	3.015333

Table S15 Coordinates of optimized geometry **[1]4**

Tag	Symbol	X	Y	Z
1	Pd	6.333781	9.539446	0.929643
2	I	6.598759	7.632104	2.777719
3	N	6.315484	10.7109	-0.72395
4	N	5.606601	10.37839	-1.72289
5	N	7.750027	11.31268	1.513507
6	N	8.45378	11.67943	2.48779
7	C	5.0288	8.557638	-0.22021
8	C	4.266316	7.412954	-0.01341
9	H	4.364465	6.857708	0.909032
10	C	3.370994	6.971936	-0.99478
11	H	2.783401	6.079667	-0.80527
12	C	3.219764	7.649932	-2.20907
13	H	2.523876	7.284552	-2.95477
14	C	3.968445	8.789871	-2.45071
15	H	3.885385	9.340704	-3.3801
16	C	4.860342	9.246804	-1.46489
17	C	7.24037	11.75984	-0.83333
18	C	7.424839	12.48584	-2.0183
19	H	6.814461	12.23947	-2.87642
20	C	8.379414	13.48656	-2.06885
21	H	8.52293	14.04782	-2.98468
22	C	9.161156	13.7711	-0.9408
23	H	9.910445	14.55281	-0.98528
24	C	8.979173	13.0644	0.236859
25	H	9.565964	13.28449	1.117295
26	C	8.017824	12.04652	0.308816
27	C	8.157849	11.21276	3.772248
28	C	6.863723	10.89074	4.207006
29	H	6.034737	10.93652	3.514325
30	C	6.654293	10.56121	5.539716
31	H	5.654329	10.31908	5.87864
32	C	7.72411	10.52304	6.43315
33	H	7.55245	10.25381	7.469085
34	C	9.014056	10.84346	6.001562
35	H	9.8433	10.81934	6.698669
36	C	9.227974	11.21533	4.682978
37	H	10.2122	11.49787	4.329152

Table S16 Coordinates of optimized geometry **^{1}PAAB**

Tag	Symbol	X	Y	Z
1	N	3.466794	0.836384	9.283283
2	N	3.064811	1.930161	8.822683
3	N	1.823455	3.789512	7.253418
4	N	1.413536	4.81976	6.66938
5	C	1.73459	-0.57353	12.84524
6	H	1.303888	-0.95724	13.76331
7	C	1.337878	0.676314	12.35732
8	H	0.601252	1.257759	12.90071
9	C	1.882257	1.178604	11.18364
10	H	1.588885	2.143737	10.7918
11	C	2.83804	0.42298	10.48662
12	C	3.734729	2.359861	7.650713
13	C	3.118681	3.363346	6.868092
14	C	0.104413	5.232984	7.027252
15	C	-0.34511	6.408529	6.416298
16	H	0.317993	6.919455	5.728097
17	C	-1.61723	6.899869	6.696577
18	H	-1.96202	7.811593	6.222413
19	C	-2.44468	6.216302	7.585335
20	H	-3.4368	6.594908	7.804301
21	C	5.001854	1.880907	7.284524
22	H	5.465727	1.128335	7.908225
23	C	5.641873	2.375671	6.159266
24	H	6.622877	2.001747	5.888399
25	C	5.025033	3.358389	5.374957
26	H	5.523514	3.73836	4.490277
27	C	3.776768	3.846688	5.72669
28	H	3.280611	4.599785	5.129222
29	C	-1.99651	5.039305	8.194872
30	H	-2.64459	4.509216	8.88407
31	C	-0.72904	4.544059	7.922558
32	H	-0.36584	3.634971	8.383723
33	C	3.236358	-0.82539	10.9762
34	H	3.977082	-1.38682	10.41896
35	C	2.683631	-1.32322	12.15307
36	H	2.992888	-2.29159	12.52934

Table S17 Coordinates of optimized geometry **^{1}Azobenzene**

Tag	Symbol	X	Y	Z
1	C	-2.94641	-0.5338	-0.00024
2	C	-1.54882	-0.59446	0.001033
3	C	-0.79341	0.569949	0.000906
4	C	-1.44105	1.815225	-0.0005
5	C	-2.83871	1.874732	-0.00181
6	C	-3.58958	0.702327	-0.00167
7	H	-3.52786	-1.44893	-0.00013
8	H	-1.05133	-1.55804	0.002124
9	H	0.288141	0.538818	0.001868
10	H	-3.31381	2.848702	-0.00292
11	H	-4.67236	0.753151	-0.00266
12	C	1.137261	4.269866	-0.00014
13	C	0.489619	5.515142	-0.00127
14	C	2.534916	4.210358	0.000726
15	C	1.245025	6.679546	-0.00149
16	H	-0.59193	5.546272	-0.00196
17	C	3.285789	5.382763	0.000515
18	H	3.010021	3.236388	0.001572
19	C	2.642617	6.618892	-0.00058
20	H	0.747542	7.643133	-0.00236
21	H	4.368565	5.331939	0.001199
22	H	3.224069	7.534015	-0.00076
23	N	-0.77739	3.069721	-0.00081
24	N	0.473595	3.015369	0.00015